A TWO-DIMENSIONAL DISCRETE-ORDINATES ANALYSIS OF THE CANDU® 9 END-SHIELD PENETRATIONS

by
K. M. Aydogdu and C.R. Boss

Atomic Energy of Canada Limited
Sheridan Science and Technology Park
Mississauga, Ontario L5K 1B2

ABSTRACT

The two-dimensional discrete-ordinates radiation transport code DORT[1] has been used to calculate neutron and gamma fluxes and corresponding dose rates through the end-shield outlet penetration of a central fuel channel in a CANDU 9 480/NU reactor. The 67-group coupled neutron-gamma library cross sections used in the analysis are based on primary ENDF/B-IV data, but with significant updates from new ENDF/B-VI data for many materials common to CANDU applications.

Three different fuel-channel configurations were analyzed:

i. the reference design of fuel-channel components;

ii. a "new" fuel-channel design, where the rolled joint area of the end-fittings was longer than the reference design by 102 mm; a corresponding 102-mm length was removed from the body of the shield plug, and the liner tube was shortened by 102 mm; and

iii. same as case (ii) above, but the steel of the shield plug was replaced by heavy-water coolant.

Calculations were made for normal steady-state full-power operation and after reactor shutdown. The neutron and gamma dose rates were calculated throughout the end shield including the plane at the outer surface of the fuelling machine tube sheet and outside the end-fittings during reactor operation. The fluxes and dose rates were compared for these three configurations to assess the effects on dose rates in the fuelling-machine vaults.

Twenty-four hours after reactor shutdown, the dose rates outside the end-fittings, that is, in the fuelling machine vaults, have contributions from

i. decay gamma rays from the ^{60}Co activation product formed from cobalt impurities in the stainless steel of the fuelling-machine side tube sheet and other end-shield components;

ii. fission-product decay gamma rays from irradiated fuel in the reactor core;

iii. prompt gamma rays from the low fission power of the core (because of fissions from delayed neutrons and photoneutrons inside the core); and

iv. activation gamma rays from corrosion and fission products deposited in the end-fittings and feeder pipes.

The neutron flux distribution through the end shield during normal operation was used to calculate the resulting ^{60}Co activity of the fuelling-machine tube sheet, the shield plug, the end-fittings, the closure plug, etc. This ^{60}Co activity was used as a source distribution in a separate DORT analysis to calculate the ^{60}Co gamma dose rates at the outer surface of the end-fittings.

The fission-product decay gamma spectrum from an ORIGEN-S[2] calculation was incorporated as a fixed source in the fuel for the DORT transport calculation to determine the fission-product decay gamma dose rates at 24 h after shutdown.

The dose rates that are due to the low fission power of the core, i.e., neutronic power of the core (~2.0×10^{-6} FP at 24 h after shutdown), were also calculated by prorating the full-power dose rates with this neutronic power fraction.

The total dose rate from these three sources, i.e., sources (i) to (iii), were summed and compared among the three proposed fuel-channel configurations. The shutdown dose rates outside the end-fittings from source (iv) were not evaluated in this paper. However, the dose rates from this source have been measured to be as high as 2 to 5 mSv/h at CANDU 6 plants.

INTRODUCTION

The end shield of a CANDU 9 reactor is a complex assembly of steel, water and fuel-channel penetrations. A calculation of the attenuation of neutron and gamma fluxes through the end shield requires a two-dimensional transport code. The attenuation of radiation through the CANDU 9 end shield was calculated using the two-dimensional discrete ordinates transport code DORT.

DORT calculations were performed for the following cases at full power:

i. the reference design of fuel-channel components;

ii. a "new" fuel-channel design, where the rolled joint area of the end-fittings was longer than the reference design by 102 mm; a corresponding 102-mm length was removed from the body of the shield plug, and the liner tube was shortened by 102 mm; and

iii. same as case (ii) above, but the steel of the shield plug was replaced by heavy-water coolant.

When the reactor is shutdown, the dose rates in the fuelling-machine vaults are due to

i. decay gamma rays from the ^{60}Co activation product formed from the cobalt impurities in the stainless steel of the fuelling-machine side tube sheet and other end-shield components;

ii. fission-product decay gamma rays from irradiated fuel in the reactor core;

iii. prompt gamma rays from the low fission power of the core (because of fissions from delayed neutrons and photoneutrons inside the core); and

iv. activation gamma rays from corrosion and fission products deposited in the end-fittings and feeder pipes.

Two more DORT runs were made to calculate shutdown dose rates outside the end-fittings from sources (i) and (ii) above. The source (iii) contribution was evaluated by prorating the dose rates during operation by the residual fission power of the reactor core at 24 hours after shutdown, viz., ~2.0×10^{-6} FP. The dose rate from this source (iii) is small.

Dose rates in the fuelling-machine vault from source (iv) were not evaluated in this study. However, these dose rates have been measured to be as high as 2 to 5 mSv/h (200 to 500 mrem/h) at the CANDU 6 plants.

For source (i), the ^{60}Co reaction rate was calculated by the DORT code in the steel material throughout the end shield including the end-fittings. The ^{59}Co contents were taken to be 700 μg/kg (700 ppm) for the calandria side tube sheet and the lattice tube; 500 μg/kg for the fuelling-machine tube sheet; 250 μg/kg in the end-fitting, shield plug, liner tube; 150 μg/kg in the homogenized carbon steel balls and water region (60/40 region). The activation gamma dose rates are dominated by the activity in the fuelling-machine tube sheet.

For source (ii), the fission-product decay gamma source was input to a separate DORT analysis from an ORIGEN-S calculation made for an average power bundle (492 kW fission power) irradiated to an average burnup of ~4,000 MW.d/Mg.U and decayed for 24 hours. The fission-product decay gamma spectrum from ORIGEN-S was converted into the DORT gamma energy group scheme.

DESCRIPTION OF CANDU 9 END SHIELD

The end shields are approximately 7.54-m-diameter discs at both ends of the reactor core. Each end shield has a 887-mm-region of carbon steel balls and light water sandwiched between a 89-mm-thick calandria side tube sheet and a 89-mm-thick fuelling-machine side tube sheet; a total thickness of 1065 mm.

In each end shield, 480 fuel-channel penetrations allow primary coolant to flow through the end shield and permit refuelling operations. The fuel channel penetrations are arranged on the 285.8-mm-square lattice of the reactor core and are formed by thin-walled lattice tubes.

The penetrations are plugged by the stainless steel end fittings that can be thought of as a thick-walled tube and shield plug assemblies. Except for a narrow gas annulus between the lattice tube and the end-fitting, the remaining volumes are filled with heavy-water coolant. The fuel-channel assembly showing the end-fitting, liner tube and shield plug is given in Figure 1. The feeder pipes were ignored in the analysis.

DORT ANALYSES

Because the 480 fuel channels form a repeating array, radiation transport through the end shield was analyzed for one fuel-channel penetration (a cell) using reflected boundary conditions simulating a repeating array.

The fuel channel was modelled in a two-dimensional R-Z geometry calculation taking into account.

i. Steady-state operations at 100% full power.

ii. A central fuel channel for which the channel power is at 6.44 MW(th).

iii. The fuel-channel assembly as shown in Figure 1.

iv. The downstream end of the fuel channel.

v. A 285.8-mm square lattice pitch as an equal area circle that has a radius of 161.2 mm in the R-Z geometry calculation.

The simplified representation of the fuel-channel penetration is shown in Figure 2. The region identifications and materials for Figure 2 are given in Table 1. A nominal fuel-channel length of 11756 mm was used. The end-fitting, liner tube and shield plug lengths were taken to be 2834 mm, 2262 mm and 981 mm respectively in the analyses. Note that the liner tube length was 102 mm shorter than this value in the DORT analysis for the new fuel-channel design.

Source Distribution.

DORT expects the radial and axial fission neutron density distribution in the source region (fuel bundle), when it is run in the fixed source mode. The source length was taken to be just over two-bundle lengths long, i.e., 990.6 mm (in-core region) and ~40 mm long (out-of core region). The latter represents the small portion of the fuel string at the downstream end of the fuel channels located in the calandria side tube sheet area, as dictated by the outlet shield plug position in the channel. The neighbouring fuel channels and bundles in the core beyond the two-bundle-long fuel string were represented using a reflective boundary condition.

Radial Fission Density Distribution (in-core region).

A 37-element fuel bundle contains a central element, an inner ring (6 elements), an intermediate ring (12 elements) and an outer ring (18 elements). In the DORT analysis, each of those rings and the central element was represented by two radial meshes. A total of 8 radial meshes were used to represent the fuel bundle.

The radial fission density distribution in the fuel bundle was based on the bundle power distribution for a bundle irradiated to an average exit burnup. The relative fission rates in the central fuel elements and the fuel rings are

i. 1.000 central element

ii. 1.052 inner ring

iii. 1.180 intermediate ring

iv. 1.428 outer ring

These values should be used with a normalization factor, which can be evaluated as follows.

Table 1
Region Identification and Region Materials
Used in DORT Model

No.	Region	Material	No.	Region	Material
1	Central Fuel Pin	UO_2 Fuel			
2	Coolant and Sheath	$Zr + H_2O$	32	Shield Plug Hole	$SS410 + H_2O$
3	Inner Fuel Annulus	UO_2 Fuel	33	Liner Tube	SS410
4	Coolant and Sheath	$Zr + H_2O$	34	Liner Tube Hole	$SS410 + H_2O$
5	Intermediate Fuel Annulus	UO_2 Fuel	35	Coolant	D_2O
6	Coolant and Sheath	$Zr + H_2O$	36	End Fitting	SS403L
7	Outer Fuel Annulus	UO_2 Fuel	37	End Fitting	SS403L
8	Coolant and Sheath	$Zr + H_2O$	38	Lattice Tube	SS304L
9	Pressure Tube	Zr	39	Annulus Gas	CO_2
10	Annulus Gas	CO_2	40	Annulus Gas	CO_2
11	Calandria Tube	Zr	41	Lattice Tube	SS304L
12	Moderator	D_2O	42	Fuelling Machine Tube Sheet	SS304L
13	Coolant	D_2O	43	Coolant	D_2O
14	Fuel Adaptor	SS410	44	Shield Plug	SS410
15	Coolant	D_2O	45	Shield Plug	SS410
16	Fuel Adaptor	SS410	46	Shield Plug	SS410
17	Coolant	D_2O	47	Coolant	D_2O
18	Calandria Side Tube Sheet	SS304L	48	Liner Tube	SS410
19	Shield Plug	SS410	49	Shield Plug	SS410
20	Annulus Gas	CO_2	50	Coolant	D_2O
21	Calandria Side Tube Sheet	SS304L	51	End-Fitting	SS403L
22	Calandria Side Tube Sheet	SS304L	52	End-Fitting	SS403L
23	Inboard Bearing	SS304L	53	End-Fitting Sleeve	SS403L
24	Carbon Steels Balls+H_2O	$SS410 + H_2O$	54	End-Fitting	SS403L
25	Annulus Gas	CO_2	55	Air	Air
26	Lattice Tube	SS304L	56	Air	Air
27	Closure	SS403L	57	Air	Air
28	Air	Air	58	End-Fitting	SS403L
29	End Fitting	SS403L	59	End-Fitting	SS403L
30	Annulus Gas	CO_2	60	End-Fitting	SS403L
31	Coolant	DO_2	61	Air	Air

If P represents a bundle thermal power in kW, P/0.9575 represents bundle fission power in kW. The factor 0.9575 is the ratio of the total thermal reactor power (2707 MW) to that of the total fission power (2827 MW) of CANDU 9 reactor.

The average fission density can be calculated using $\frac{P \times 6.242 \times 10^{15}}{0.9575 \times 206.1 \times 2121.3} = 1.491 \times 10^{10} \times P$ fissions.cm^{-3}.s^{-1},

where 6.242×10^{15} = MeV/s per kW

206.1 = MeV/fission

2121.3 = Volume of 37 fuel elements based on 49.53-cm bundle length and a fuel element radius of 0.607 cm in cm^3.

The average of the radial power distribution values is equal to 1.275, i.e. (1.000 + 6 x 1.052 + 12 x 1.180 + 18 x 1.428)/37. Consequently, the radial power distribution values are

i. central element: $1.491 \times 10^{10} P \times \frac{1.000}{1.275} = 1.170 \times 10^{10} P$

ii. inner ring: $1.491 \times 10^{10}\ P \times \frac{1.052}{1.275} = 1.230 \times 10^{10} P$

iii. intermediate ring: $1.491 \times 10^{10}\ P \times \frac{1.180}{1.275} = 1.380 \times 10^{10} P$

iv. outer ring: $1.491 \times 10^{10}\ P \times \frac{1.428}{1.275} = 1.670 \times 10^{10} P$

The radial factors incorporated into the DORT calculations are 1.170×10^{10}, 1.230×10^{10}, 1.380×10^{10} and 1.670×10^{10} in units of fissions.cm^{-3}.s^{-1} per kW thermal power. This means that the axial source distribution should be given as kW thermal power in a fuel bundle.

Axial Fission Density Distribution (in-core region).

The axial power distribution was specified in terms of fissions.cm^{-3}.s^{-1} per kW thermal power along the fuel string at the mesh mid-points (14 meshes) of the DORT calculations. This was based on the fission density distribution from an ANISN[3] end-shield analysis. The axial source distribution used in the analysis is given in Tables 2 and 3.

Table 2
Axial Power Shape Used in DORT Calculations

Mesh #	Mesh Mid-point in Coordinate System of Figure 2 (cm)	Bundle Thermal Power (kW)
1	-95.5	510
2	-88.5	480
3	-81.4	456
4	-74.3	422
5	-67.2	390
6	-60.1	356
7	-53.1	321
8	-46.0	285
9	-38.9	247
10	-31.8	209
11	-24.8	171
12	-17.7	132
13	-10.6	92
14	-3.5	49

Radial and Axial Fission Density Distribution for Fuel in the Core and in the End Shield Region.

Using the axial and radial source distribution given above, DORT was run to calculate the fission density distribution in the out-of-core region of the fuel string (~ 40 mm), represented by axial mesh numbers 15 to 21 and radial mesh number sets (1, 2), (5, 6), (9,10) and (13, 14). The fission densities were normalized to those at axial mesh 14 (see Table 3). The source distribution in the out-of-core region was added to the fission density distribution in the first 14 axial meshes (in-core region) to obtain the fission density distribution over the entire problem. Subsequent DORT runs were made with the fuel in the core and in the end shield region.

Table 3
Normalized Axial and Radial Fission Density Distribution used in DORT Calculation (out-of-core region of fuel)

Axial Mesh No.	Axial Mesh Mid-Point (cm)	Radial Mesh No. 1, 2	Radial Mesh No. 5, 6	Radial Mesh No. 9, 10	Radial Mesh No. 13, 14
14	-3.54	1.000	1.000	1.000	1.000
	0.0[a]				
15	0.30	0.638	0.626	0.610	0.589
16	0.90	0.561	0.550	0.528	0.504
17	1.51	0.489	0.485	0.455	0.431
18	2.11	0.428	0.420	0.392	0.363
19	2.80	0.371	0.360	0.330	0.298
20	3.57	0.322	0.308	0.271	0.237
21	4.01	0.304	0.287	0.243	0.207
	4.06[a]				

[a] Zero represents core/calandria tube sheet boundary; 4.06 cm = distance into end shield.

Input Data on Group Structure, Angular Quadrature Materials and Mesh Structure

Tables 4 and 5 show the energy structure of the 67-group coupled neutron-gamma library of cross sections used in the calculation. There are 47 neutron energy groups that include 19 fast neutron groups ($E_n \geq 0.82$ MeV), 26 intermediate neutron groups (0.82 MeV > E_n > 0.414 eV) and two thermal neutron groups ($E_n \leq 0.414$ eV). There are 20 gamma groups. Table 4 also shows the fission neutron spectrum. The number of neutrons per fission was taken to be 2.626.

Cross sections in the ANISN library were represented by a Legendre expansion limited to P_3. The GIP code, which is a pre-processor code for DORT, was used to prepare a group-independent cross-section library. The microscopic cross sections from the library have been mixed using GIP to obtain the macroscopic cross sections for the materials in Table 6. Note that the library is fully coupled and includes gamma production from neutron interactions as part of the downscatter matrix of cross sections. The cross sections for ^{235}U and ^{238}U from the library include fission-product decay gammas.

An S_{16} angular quadrature with 160 angular directions was used[4] in the calculations. The θ-weighted flux model was used to extrapolate the angular fluxes across each mesh, as recommended by Reference 1.

RESULTS & DISCUSSION

The neutron fluxes, and the neutron and gamma dose rates through the CANDU 9 end shield associated with a central fuel-channel were calculated by the two-dimensional DORT code. DORT was run for the original (reference) fuel-channel design with no changes in the shield plug, end-fitting and liner tube arrangements; a new fuel-channel design where the rolled joint area of the end-fittings was taken to be longer than the reference design by 102 mm, a corresponding 102-mm length was removed from the body of the shield plug, and the liner tube was shortened by 102 mm; and with the new fuel-channel design but with the shield plug absent.

The radial distributions of the fast, intermediate and thermal neutron fluxes at the outer surface of the fuelling-machine tube sheet and at the end of the end-fittings ("E" face) are shown in Figure 3 for the new fuel-channel design during steady-state operations at 100% full power. The fluxes are lowest with the shield plug missing case (not shown), because the coolant is a better neutron attenuator than steel. The fluxes with the new fuel-channel design are also lower than were those for the original design. The comparison of neutron fluxes and neutron and gamma dose rates is shown in Table 7. The current 67-group library overpredicts the thermal flux population at energies below 0.1 eV in D_2O. This has resulted in slight overestimation of the thermal neutron fluxes given in Figure 3. The new library under development removes the 0.1 eV boundary.

Table 4
The Upper Limit and Mean Energies for 47 Neutron Groups
and Fission Neutron Spectrum Used in DORT

Group	Upper Energy Limit E_u (eV)	Mean Energy $\bar{E}$ (eV)	Fraction of Neutrons per Fission	Three Group Structure
1	1.7333 E7	1.527 E7	1.4352 E-4	
2	1.4191 E7	1.305 E7	5.2801 E-4	
3	1.2214 E7	1.087 E7	2.9959 E-3	
4	1.0000 E7	9.237 E6	6.5866 E-3	
5	8.6071 E6	7.959 E6	1.4761 E-2	
6	7.4082 E6	6.635 E6	4.2101 E-2	Group I
7	6.0653 E6	5.475 E6	8.0028 E-2	(fast)
8	4.9660 E6	4.309 E6	2.0967 E-1	
9	3.6788 E6	3.288 E6	1.9981 E-1	
10	3.0119 E6	2.862 E6	1.1455 E-1	
11	2.7253 E6	2.595 E6	1.2151 E-1	
12	2.4660 E6	2.413 E6	5.2130 E-2	
13	2.3653 E6	2.355 E6	1.0480 E-2	
14	2.3457 E6	2.290 E6	6.3364 E-2	
15	2.2313 E6	2.082 E6	1.9145 E-2	
16	1.9205 E6	1.772 E6	1.8733 E-1	
17	1.6530 E6	1.489 E6	2.3326 E-1	
18	1.3534 E6	1.174 E6	3.0044 E-1	
19	1.0026 E6	8.936 E5	1.6428 E-1	
20	8.2085 E5	7.799 E5	7.1581 E-2	
21	7.4274 E5	6.679 E5	1.2345 E-1	
22	6.0810 E5	5.512 E5	9.9671 E-2	
23	4.9787 E5	4.333 E5	1.1123 E-1	
24	3.6883 E5	3.307 E5	5.7174 E-2	
25	2.9718 E5	2.377 E5	8.0717 E-2	Group II
26	1.8316 E5	1.442 E5	4.1779 E-2	(intermediate)
27	1.1109 E5	8.778 E4	2.0264 E-2	
28	6.7379 E4	5.328 E4	9.7035 E-3	
29	4.0868 E4	3.615 E4	2.7467 E-3	
30	3.1828 E4	2.888 E4	1.5871 E-3	
31	2.6058 E4	2.510 E4	4.8644 E-4	
32	2.4176 E4	2.302 E4	5.7181 E-4	
33	2.1875 E4	1.832 E4	1.5519 E-3	
34	1.5034 E4	1.065 E4	1.4015 E-3	
35	7.1017 E3	5.043 E3	4.4803 E-4	
36	3.3546 E3	2.300 E3	1.5123 E-4	
37	1.5846 E3	9.119 E2	6.5785 E-5	
38	4.5400 E2	3.212 E2	9.0896 E-6	
39	2.1445 E2	1.517 E2	3.3144 E-6	
40	1.0130 E2	6.444 E1	1.4617 E-6	
41	3.7267 E1	2.144 E1	4.3357 E-7	
42	1.0677 E1	7.558 E0	5.8265 E-8	
43	5.0435 E0	3.215 E0	3.2764 E-8	
44	1.8554 E0	1.314 E0	1.0061 E-8	
45	8.7642 E-1	6.210 E-1	4.7523 E-9	
46	4.1399 E-1	2.570 E-1	3.2268 E-9	Group III
47	1.0000 E-1	5.000 E-2	1.0277 E-9	(thermal)
	1.0000 E-5[a]			
		Total:	2.626	

[a] Lower energy limit for Group 47.

Figure 4 shows the neutron and gamma dose rates at the outer surface of the fuelling-machine tube sheet and the end of the end-fittings for the new fuel-channel design during normal operation. Figures 5 and 6 show the corresponding dose rates for the other two cases. The dose rates with the new fuel-channel design are lower than were those with the original (reference) design.

Figure 7 shows the shutdown dose rates from ^{60}Co activation gammas of the end shield components and the fission-product decay gammas from fuel in the core at 24 h after reactor shutdown for the new fuel-channel design. The total dose rate is a maximum of about 0.80 mSv/h (80 mrem/h) in the plane of the outer surface of the fuelling-machine tube sheet, but drops to 0.07 mSv/h (7 mrem/h) in the end-plane of the end-fittings.

Table 5
The Upper Limit and Mean Energies for 20 Gamma Groups
Used in DORT Calculations

Group	Upper Energy Limit E_u (eV)	Mean Energy $\bar{E}$ (eV)
48	1.40 E7	1.20 E7
49	1.00 E7	9.00 E6
50	8.00 E6	7.50 E6
51	7.00 E6	6.50 E6
52	6.00 E6	5.50 E6
53	5.00 E6	4.50 E6
54	4.00 E6	3.50 E6
55	3.00 E6	2.50 E6
56	2.00 E6	1.75 E6
57	1.50 E6	1.25 E6
58	1.00 E6	9.00 E5
59	8.00 E5	7.50 E5
60	7.00 E5	6.50 E5
61	6.00 E5	5.00 E5
62	4.00 E5	3.00 E5
63	2.00 E5	1.50 E5
64	1.00 E5	8.00 E4
65	6.00 E4	4.50 E4
66	3.00 E4	2.50 E4
67	2.00 E4 1.00 E4[a]	1.50 E4

[a] Lower energy limit for Group 67.

The thermal activation cross section for ^{59}Co given in the 67-group library overemphasizes the magnitude of cross section for the last thermal group (group 47), due to a uniform "flat" spectral weighting of the thermal cross sections. To compensate for this assumption, ^{60}Co dose rates calculated above include a scaling-down factor of 0.25.

In calculating the ^{60}Co dose rates, a "cylindrical" rather than "reflected" boundary condition was used. The former condition is considered a better simulation of a regular array of channel penetrations at the outer boundary. It ensures that the outward flux is truly independent of the cosine of the angle between the direction of travel and the R-axis. The reflected condition tends to overestimate the dose rates for arrangements involving air transport in a repeating array.

Note that the dose rate from the residual fission power of the core was estimated to be a maximum of about 2 μSv/h (0.2 mrem/h), i.e., [dose rates from Figure 4] x ~2.0 x 10^{-6}, which is the residual fission power fraction of the core at 24 hours after shutdown. The total dose rate is still a maximum of ~0.07 mSv/h. This is lower than the design criterion of 0.25 mSv/h (25 mrem/h) at 24 hours after shutdown outside the feeder cabinet. More than 80% of this shutdown field is due to the ^{60}Co activation gamma rays from the fuelling-machine tube sheet, where the cobalt impurity level in the steel was taken to be 500 μg/kg (500 ppm).

The average dose rate over one lattice pitch square was estimated to be ~0.05 mSv/h (5 mrem/h). It should be noted that these shutdown dose rates are conservative, because the effect of the feeder piping was not considered: the operating bundle powers for the neighbouring fuel channels were taken to be the same as those of the central channel, i.e., radial form factor at the end of the core was taken to be one. The radial form factor would reduce the dose rate averaged over the end shield by a factor of about 1.4. The yoke and stud assemblies of the fuel channels were also not considered in the model.

Table 6
Element Atomic Densities for the Materials Used in GIP Calculation

#	Material	Element	Atomic Density [(atoms/cm^3) x 10^{24}]
1	Stainless Steel 304: (ρ = 7.9 g/cm^3)	C Si Cr Mn Fe Ni	1.387 E-4 1.271 E-3 1.734 E-2 1.732 E-3 5.812 E-2 8.107 E-3
2	Stainless Steel 403L (ρ = 7.9 g/cm^3)	C Si Cr Mn Fe Ni	4.753 E-4 4.235 E-4 1.107 E-2 5.196 E-4 7.384 E-2 2.026 E-4
3	Stainless Steel 410 (ρ = 7.9 g/cm^3)	Si Cr Mn Fe	1.670 E-3 1.080 E-2 8.550 E-4 7.220 E-4
4	Carbon Steel Ball and Water (60/40 Region)	H C O Si Mn Fe	2.674 E-2 7.794 E-4 1.337 E-2 2.525 E-4 5.010 E-4 5.002 E-2
5	Zirconium (ρ = 6.55 g/cm^3)	Zr	4.325 E-2
6	Moderator (ρ = 1.09 g/cm^3)	H D O	1.839 E-4 6.599 E-2 3.309 E-2
7	Coolant (ρ = 0.82 g/cm^3)	H D O	1.384 E-4 4.964 E-2 2.489 E-2
8	UO_2 Fuel (ρ = 10.67 g/cm^3)	O U-235 U-238	4.758 E-2 1.713 E-4 2.362 E-2
9	Coolant and Sheath	H D O Zr	1.152 E-5 4.130 E-2 2.071 E-2 7.264 E-3
10	Air[a]	O	5.018 E-5
11	Annulus Gas (CO_2)	C O	2.879 E-5 5.758 E-5
12	Coolant and Liner Tube	H D O Si Cr Mn Fe	4.408 E-5 1.581 E-2 7.928 E-3 1.138 E-3 7.360 E-3 5.827 E-4 4.920 E-4
13	Coolant and Shield Plug	H D C Si Cr Mn Fe	4.002 E-5 1.435 E-2 7.197 E-3 1.187 E-3 7.677 E-3 6.078 E-4 5.132 E-4

[a] Treated as oxygen.

Table 7
Comparison of Neutron Fluxes and Neutron and Gamma Dose Rates Calculated by the DORT code for the Original Fuel-Channel, New Fuel-Channel and New Fuel-Channel (no shield plug) Designs

Fast, Intermediate and Thermal Neutron Fluxes ($n.cm^{-2}.s^{-1}$) and Neutron and Gamma Dose Rates (mrem/h)		Fuelling-Machine Tube-Sheet Outer Surface			At the End of End-Fittings		
		Original Fuel Channel	New Fuel Channel	New Fuel Channel (no shield plug)	Original Fuel Channel	New Fuel Channel	New F/C (no shield plug)
Φ_f	channel axis	3.48E6[a]	2.26E6	3.22E5	2.80E4	1.75E4	4.05E3
Φ_f	mid-lattice	5.37E6	3.63E6	3.49E5	4.07E4	2.54E4	5.88E3
Φ_f	lattice edge	1.51E6	9.69E5	2.24E5	4.45E5	2.84E5	7.16E4
Φ_{int}	channel axis	1.05E8	7.15E7	7.56E6	6.20E5	4.05E5	6.40E4
Φ_{int}	mid-lattice	1.04E8	7.16E7	6.99E6	7.87E5	5.15E5	8.05E4
Φ_{int}	lattice edge	2.69E7	1.80E7	2.45E6	6.67E6	4.44E6	6.54E5
Φ_{th}	channel axis	4.09E7	2.84E7	4.64E6	1.12E4	7.55E3	9.98E2
Φ_{th}	mid-lattice	2.91E7	2.03E7	3.17E6	1.70E4	1.16E4	1.52E3
Φ_{th}	lattice edge	2.95E6	2.03E6	2.68E5	5.54E5	3.80E5	5.21E4
D_n	channel axis	6.78E5	4.52E5	5.87E4	6.29E3	3.99E3	8.01E2
D_n	mid-lattice	8.60E5	5.86E5	5.91E4	8.28E3	5.26E3	1.06E3
D_n	lattice edge	2.57E5	1.67E5	3.24E4	7.26E4	4.69E4	1.00E4
D_γ	channel axis	5.34E5	4.40E5	4.58E5	8.62E2	6.25E2	4.17E2
D_γ	mid-lattice	6.74E5	5.38E5	6.89E5	1.72E3	1.27E3	1.03E3
D_γ	lattice edge	7.05E4	5.20E4	3.09E4	3.08E4	2.35E4	2.17E4

[a] read 3.48E6 as 3.48×10^6.

A comparison of the fuel channel configurations has shown that the "new" fuel-channel design is acceptable from a shielding viewpoint. Of particular interest is the finding that the dose rates are lowest with the steel of the shield plug replaced with heavy water, i.e., fuel-channel configuration (iii). This implies that a fuel-handling scenario in which the shield plug cannot be replaced at the inlet end would be acceptable.

It should be noted that if the option of removing the shield plugs needs to be pursued, then more rigourous Monte Carlo calculations should be used to confirm the findings from the DORT analysis.

REFERENCES

1. "TORT-DORT, Two- and Three-Dimensional Discrete Ordinates Transport Code, Version 2.12.14", Oak Ridge National Laboratory Report CCC-543, 1995 January.
2. HERMANN, O.W. and WESTFALL, R.M., "ORIGEN-S –SCALE System Module to Calculate Fuel Depletion, Actinide Transmutation, Fission Product Build-up and Decay, and Associated Radiation Source Terms", Oak Ridge National Laboratory (1993, November).
3. ENGLE, Jr. W.W., "A Users Manual for ANISN – A One Dimensional Discrete Ordinates Transport Code with Anisotropic Scattering", K-1693, Union Carbide Corporation (March 1967).
4. JENAL, J.P., et al., "The Generation of a Computer Library for Discrete Ordinates Quadrature Sets", Oak Ridge National Laboratory ORNL/TM-6023 (October, 1977)

Figure 1
Fuel-Channel Assembly

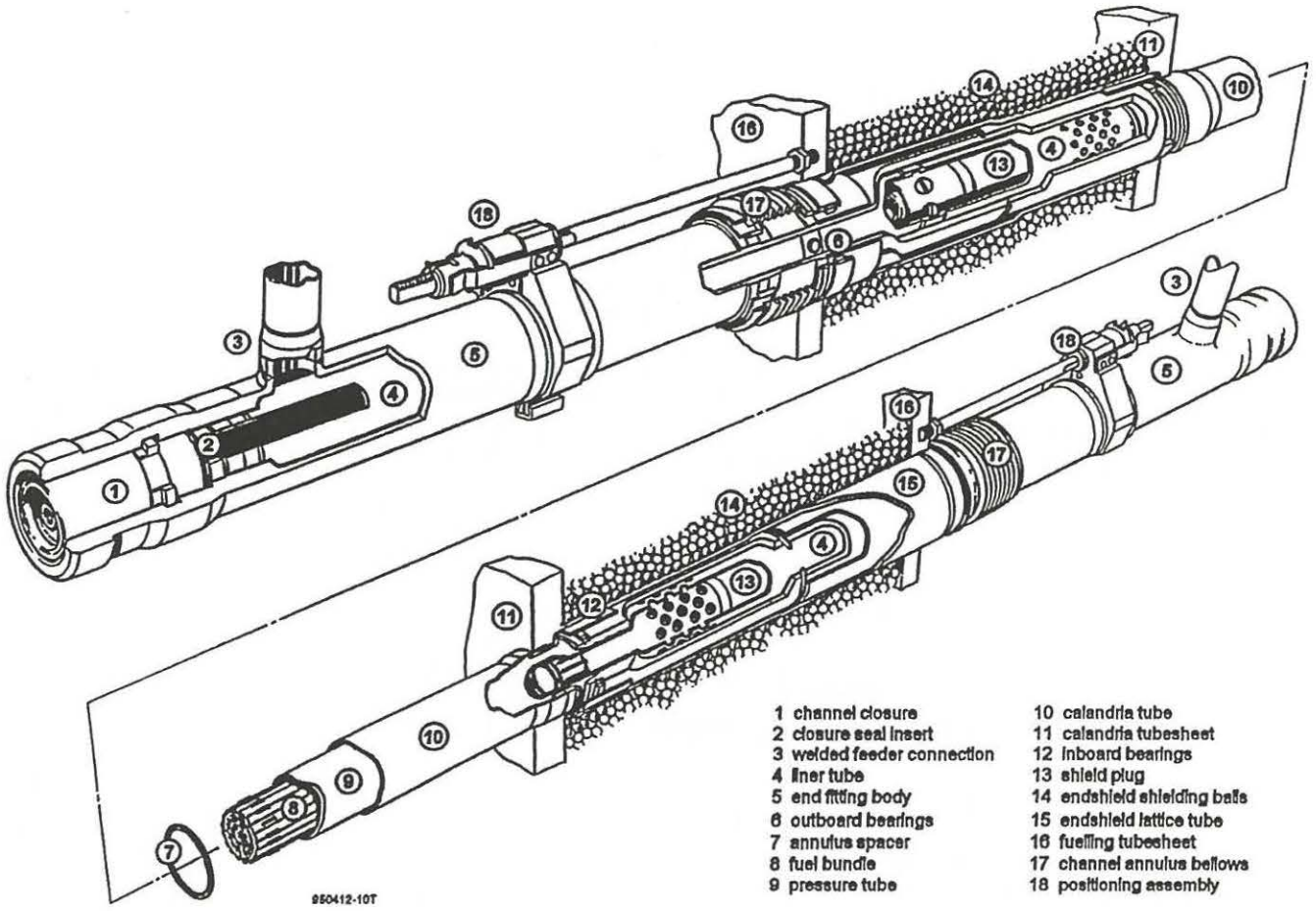

Figure 2
DORT Model Used for Analysis of the CANDU 9 End-Shield
Associated with a Central Fuel Channel (model for new fuel-channel design)

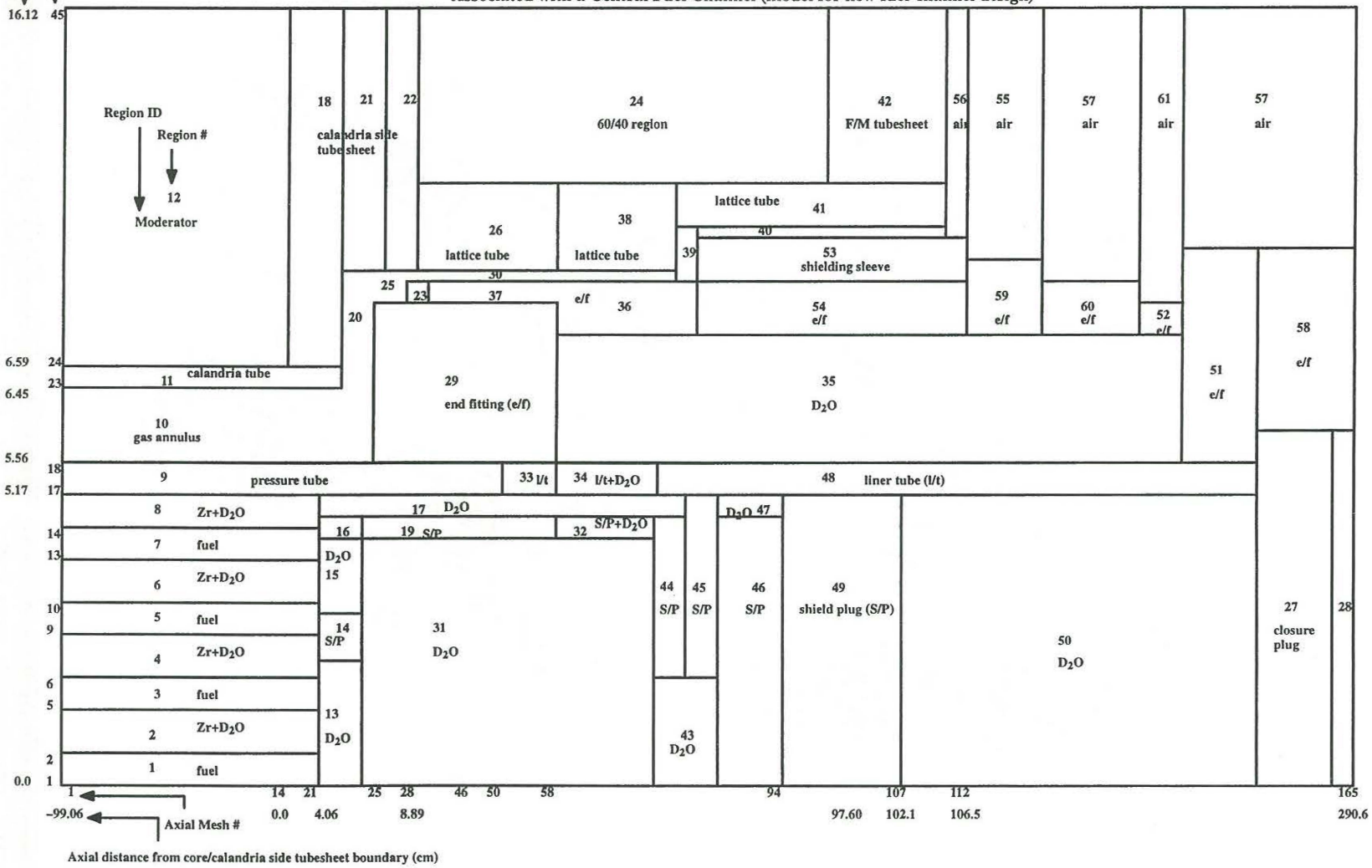

Figure 3

Neutron Fluxes in the Plane of the Outer Surface of the Fuelling-Machine Tube Sheet and in the End-Plane of the End-Fitting during Reactor Operation (new fuel-channel design)

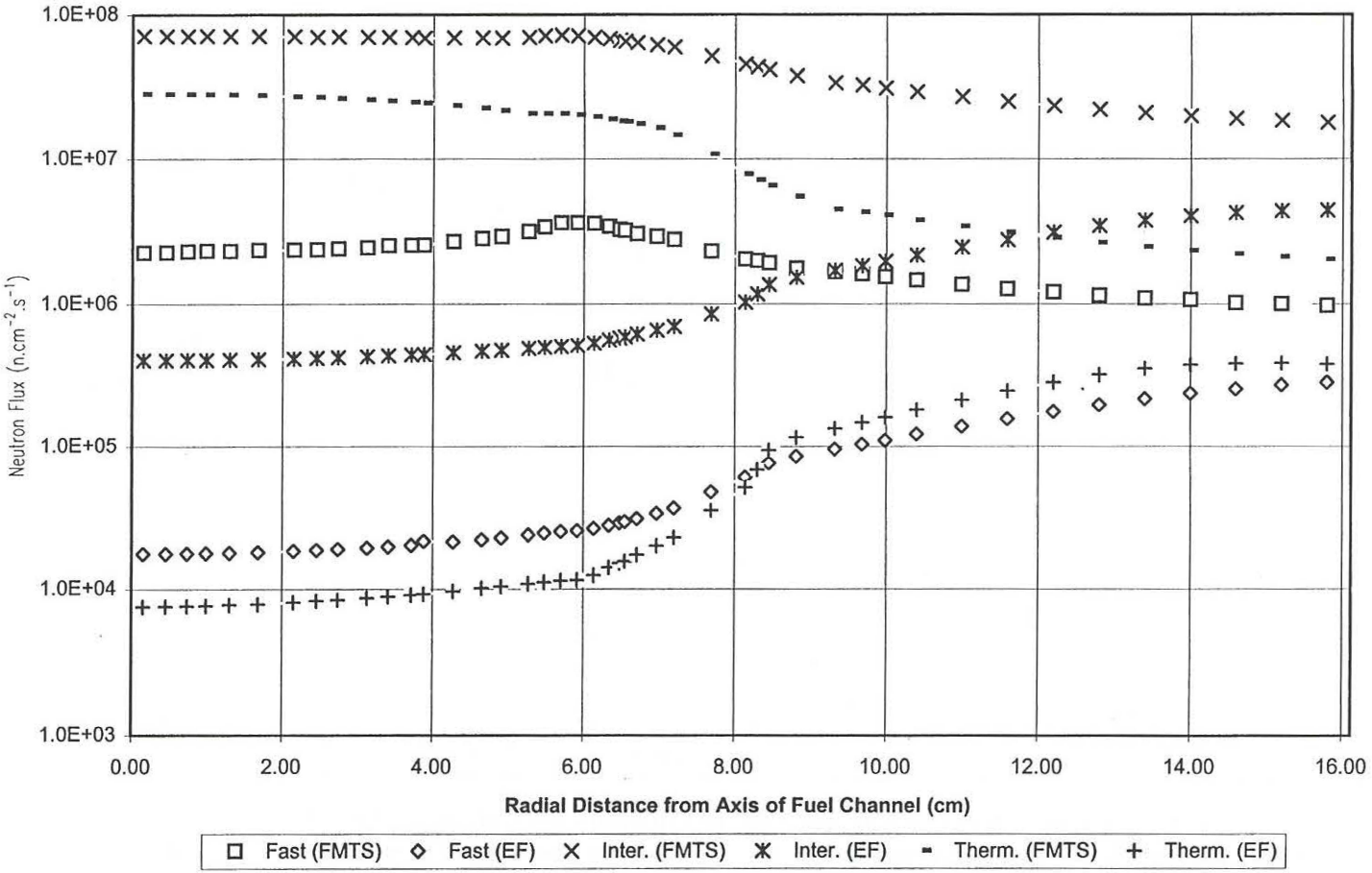

Figure 4
Neutron and Gamma Dose Rate in the Plane of the Outer Surface of the Fuelling-Machine Tube Sheet and in the End-Plane of the End-Fitting during Reactor Operation (reference fuel-channel design)

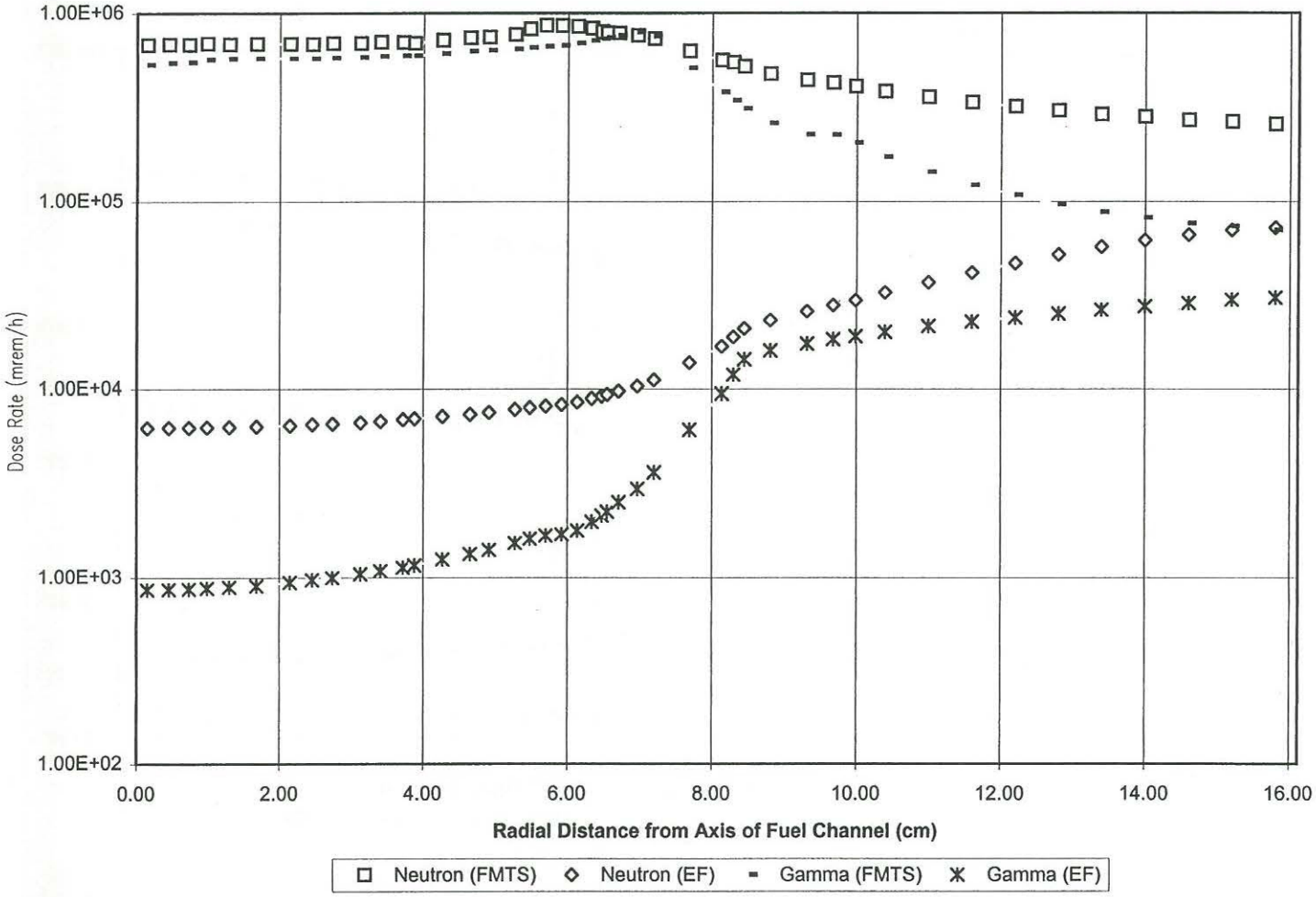

Figure 5

Neutron and Gamma Dose Rate in the Plane of the Outer Surface of the Fuelling-Machine Tube Sheet and in the End-Plane of the End-Fitting during Reactor Operation (new fuel-channel design)

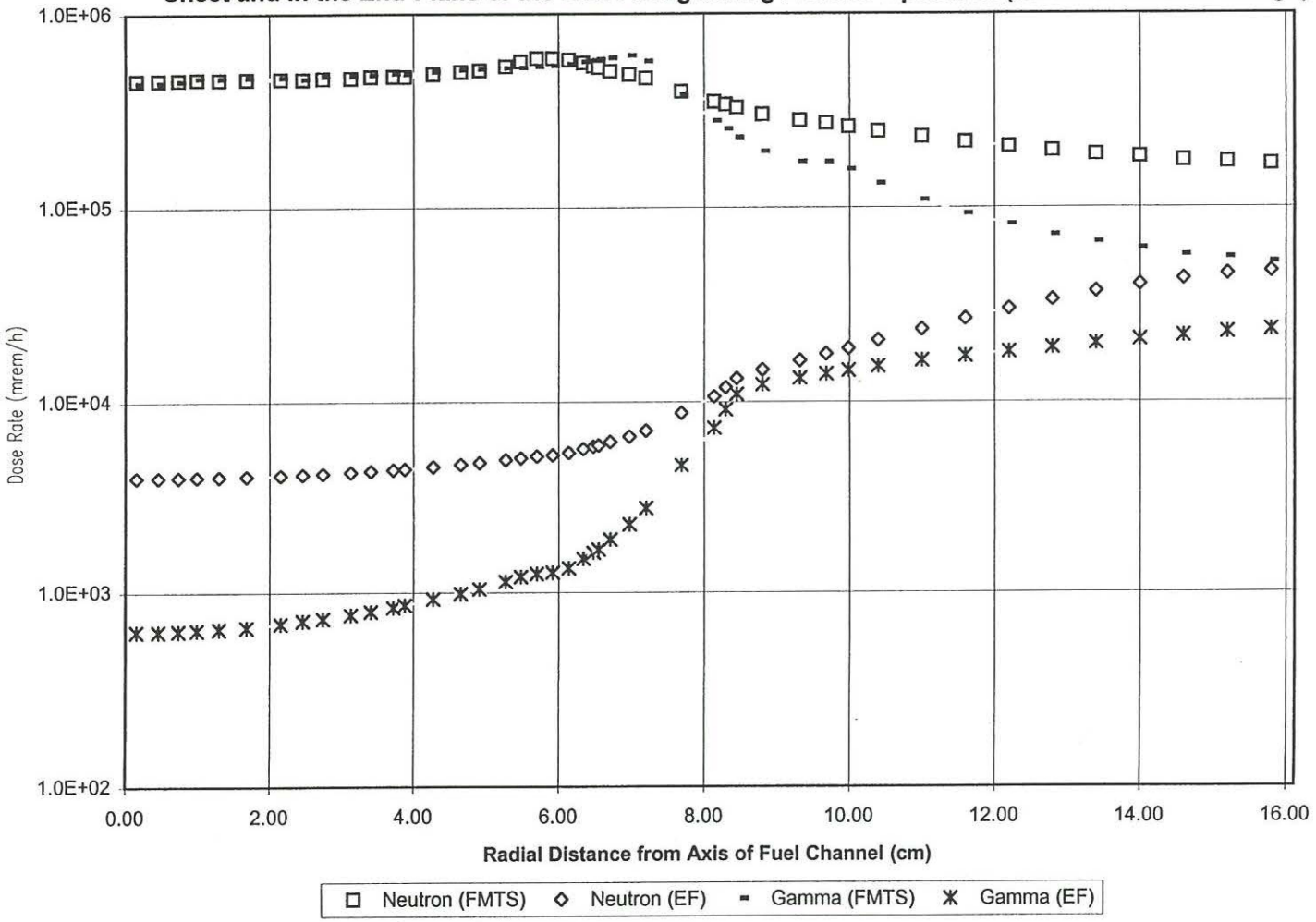

Figure 6

Neutron and Gamma Dose Rate in the Plane of the Outer Surface of the Fuelling-Machine Tube Sheet and in the End-Plane of the End-Fitting during Reactor Operation (new fuel-channel with no shield plug in channel)

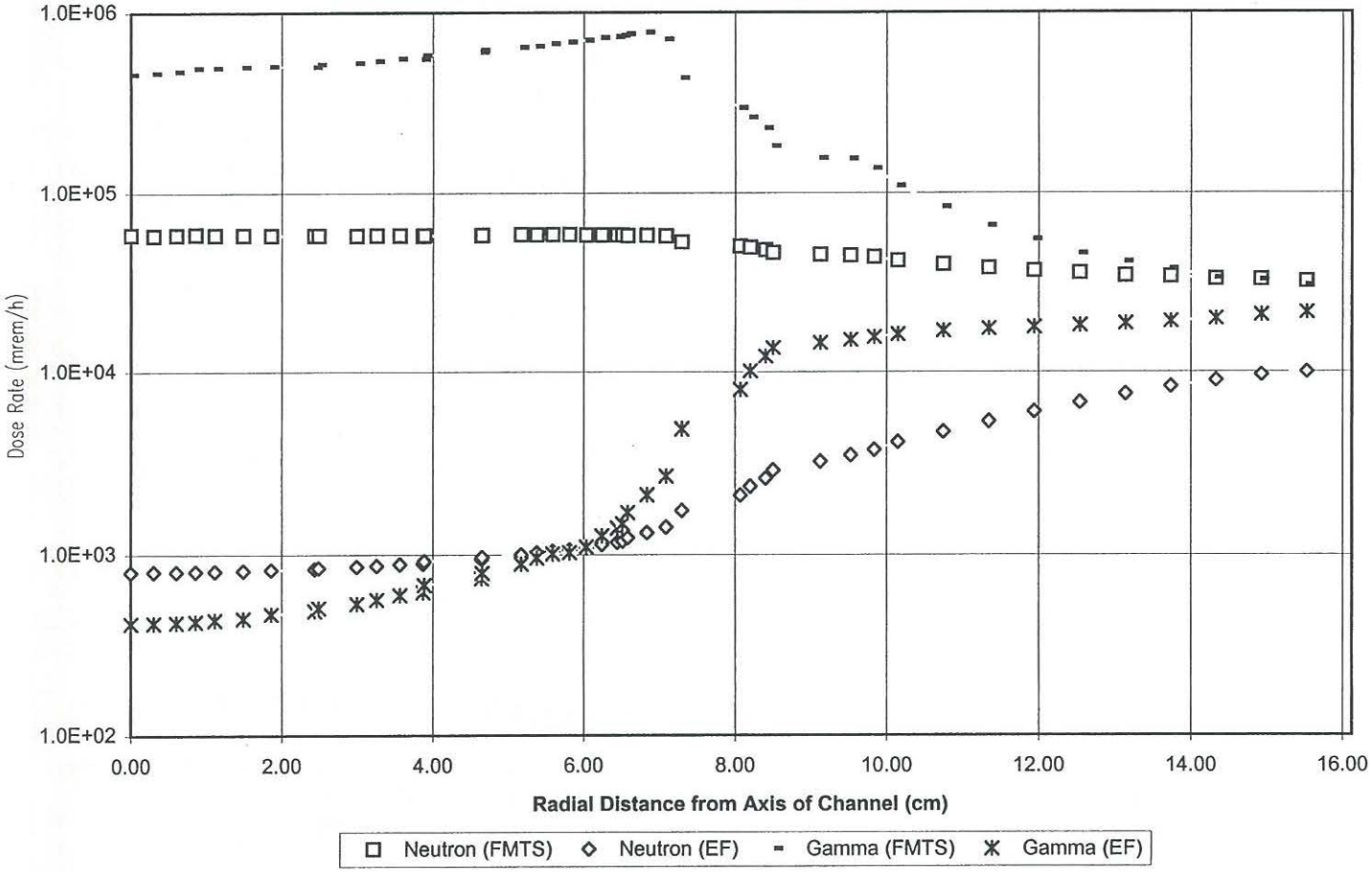

Figure 7

Cobalt-60 and Fission-Product Decay Gamma Dose Rate in the Plane of the Outer Surface of the Fuelling-Machine Tube Sheet and in the End-Plane of the End-Fitting at 24 h after Shutdown (new fuel-channel design)